



Originally published as:

Matzka, J., Siddiqui, T., Lilienkamp, H., Stolle, C., Veliz, O. (2017): Quantifying solar flux and geomagnetic main field influence on the equatorial ionospheric current system at the geomagnetic observatory Huancayo. - *Journal of Atmospheric and Solar-Terrestrial Physics*, 163, pp. 120—125.

DOI: <http://doi.org/10.1016/j.jastp.2017.04.014>

1 **Quantifying solar flux and geomagnetic main field influence on the equatorial**
2 **ionospheric current system at the geomagnetic observatory Huancayo**

3

4 Jürgen Matzka^a, Tarique A. Siddiqui^{a,b}, Henning Lilienkamp^b, Claudia Stolle^{a,b}, Oscar
5 Veliz^c

6

7 ^aGFZ German Research Centre for Geosciences, 14473 Potsdam, Germany

8 juergen.matzka@gfz-potsdam.de

9

10 ^bInstitute of Earth and Environmental Sciences, University of Potsdam, 14469 Potsdam,
11 Germany

12

13 ^cInstituto Geofísico del Perú, Jicamarca Radio Observatory, Lima, Peru

14

15 Corresponding author: Jürgen Matzka, juergen.matzka@gfz-potsdam.de

16

17 Published in 2017 in Journal of Atmospheric and Solar-Terrestrial Physics

18 <http://dx.doi.org/10.1016/j.jastp.2017.04.014>

19

20 **Abstract**

21 In order to analyse the sensitivity of the equatorial ionospheric current system, i.e. the
22 solar quiet current system and the equatorial electrojet, to solar cycle variations and to
23 the secular variation of the geomagnetic main field, we have analysed 51 years (1935 to
24 1985) of geomagnetic observatory data from Huancayo, Peru. This period is ideal to
25 analyse the influence of the main field strength on the amplitude of the quiet daily
26 variation, since the main field decreases significantly from 1935 to 1985, while the
27 distance of the magnetic equator to the observatory remains stable. To this end, we
28 digitised some 19 years of hourly mean values of the horizontal component (H), which
29 have not been available digitally at the World Data Centres. Then, the sensitivity of the
30 amplitude ΔH of the quiet daily variation to both solar cycle variations (in terms of
31 sunspot numbers and solar flux F10.7) and changes of the geomagnetic main field
32 strength (due to secular variation) was determined. We confirm an increase of ΔH for
33 the decreasing main field in this period, as expected from physics based models

34 (Cnossen, 2016), but with a somewhat smaller rate of 4.4 % (5.8 % considering one
35 standard error) compared with 6.9 % predicted by the physics based model.

36 **Keywords**

37 Magnetic field; equatorial ionosphere; geomagnetic secular variation; solar cycle

38

39 **Introduction**

40 On time scales of decades to centuries, the thermosphere and ionosphere have
41 undergone long-term changes like cooling and contraction. Possible drivers discussed in
42 the literature are changes in greenhouse gases or the geomagnetic main field and the
43 forcing from the lower atmosphere as well as long-term trends in solar activity and
44 geomagnetic activity (e.g. Cnossen, 2012; Cnossen, 2016). To better understand these
45 long-term changes in the upper atmosphere, it is important to know the sensitivity of
46 the system to the secular variation of the geomagnetic field as well as changes in solar
47 flux. There are two ways to study long-term trends. One is by modelling the physics of
48 the coupled thermosphere-ionosphere-magnetosphere system by using geomagnetic
49 main field models at different epochs to introduce a time dependency and by taking into
50 account different solar activity levels, parameterised by the F10.7 solar flux index (e.g.
51 Cnossen et al., 2012; Cnossen and Richmond, 2013; Cnossen and Matzka, 2016). The
52 other approach is by analysing homogenous time series of observations that are
53 sensitive to ionospheric processes such as geomagnetic observatory data (e.g. Sellek,
54 1980; Schlapp et al., 1990; Macmillan and Droujinina, 2007; de Haro Barbas et al., 2013,
55 Shinbori et al., 2014).

56

57 The quiet daily variation at a station close to the magnetic equator (defined as the line
58 around the globe with geomagnetic inclination $I = 0^\circ$ or vertical component of the
59 geomagnetic field $Z = 0$ nT) combines contributions from the solar quiet (Sq) current
60 system and the equatorial electrojet (EEJ). The EEJ is a current ribbon (e.g. Chapman,
61 1951; Marriot et al., 1979; Stening, 1985, Lühr et al., 2004) limited to a few degrees in
62 latitude along the magnetic equator. Since both the Sq currents at low latitudes and the
63 EEJ current system are east-west oriented, their magnetic field at ground level is
64 oriented northerly and simply adds to the horizontal component of the geomagnetic
65 field H. Hence the H component is usually studied to quantify Sq and EEJ at the equator.
66 The Sq and EEJ currents and their magnetic effects are assumed to be zero during night
67 time and they assume a maximum at local noon (corresponding to 17:00 UT at HUA).

68

69 In order to study the effect of the secular variation of the Earth's magnetic field on the
70 strength of the equatorial ionospheric current systems, we investigate the amplitude of
71 the magnetic variation measured at Huancayo, Peru. The geomagnetic observatory
72 Huancayo (IAGA code HUA, latitude -12.05° , longitude 284.67° , geomagnetic inclination I
73 $=-0.53^\circ$ in 2017, operated by Instituto Geofísico del Perú) has been very close to the
74 magnetic equator since it was established in 1922. This is expressed by its consistently
75 small geomagnetic inclination (Fig. 1a). At the same time, the geomagnetic field strength
76 has decreased considerably in the region during this period due to secular variation (Fig.
77 1b). Indeed, this is the strongest decrease in geomagnetic field strength observed at any
78 location where the magnetic equator remained stationary over the last 100 years or so
79 (see, e.g. Figure 1 and Figure 2 in Cnossen and Richmond, 2013). For our investigation,
80 we had to digitise significant amounts of handwritten data to fill in data gaps in the
81 existing digital datasets for Huancayo.

82

83 A scaling law has recently been derived by Cnossen (2016) that predicts that the daily
84 magnetic variation of the H component at the magnetic equator is proportional to $M^{-0.7}$,
85 with M being the dipole moment of the Earth's magnetic field. This is based on results by
86 a Coupled Magnetosphere-Ionosphere-Thermosphere (CMIT) model (Cnossen et al,
87 2012) which consists of a magneto-hydrodynamic magnetosphere model and the
88 Thermosphere-Ionosphere-Electrodynamics General Circulation Model (TIE-GCM) and
89 is in agreement with an earlier scaling law for the Cowling conductance (Glassmeier,
90 2004). We will compare our analysis of Huancayo data to the physics-based approach by
91 Cnossen (2016). Note that for model-based studies often a simple dipole geomagnetic
92 field is used, for which the local geomagnetic field strength F everywhere scales linearly
93 with dipole moment. The Earth's magnetic field, however, is more complex, and
94 therefore we compare the quiet daily variation with the field strength F at Huancayo
95 rather than the dipole moment M .

96

97 **Material and Methods**

98 Geomagnetic ground data come with different levels of quality, calibration and time
99 resolution. Data from geomagnetic observatories have the highest level of quality and
100 are absolutely calibrated (e.g. Matzka et al., 2010, Chulliat et al., 2016). These data can be
101 used to study secular variation (the slow changes of the geomagnetic main field due to

102 processes in the core of the Earth) as well as long-term trends in the magnetic signature
103 of ionospheric and magnetospheric currents (e.g. Cnossen and Richmond, 2013). For
104 secular variation studies, annual means of observatory data already contain the major
105 information of its variability, while ionospheric or magnetospheric studies typically
106 require hourly mean values or minute means, e.g. to properly describe daily and
107 seasonal variations. For the geomagnetic observatory HUA, which is operated since
108 1922, there exists a continuous series of annual means, but there are significant gaps in
109 data coverage for hourly mean values at the World Data Centres in the 1960ies to mid
110 1980ies (see Fig. 1 d). The hourly mean values in the period considered here (1935 to
111 1985) were produced with the original instrument installed at Huancayo in 1922, the
112 Eschenhagen-type magnetograph DTM CIW Nr. 2 with a photographic recorder by Otto
113 Toepfer und Sohn, Potsdam (Choque et al., 2014).

114

115 We have digitised existing scans of the handwritten, monthly tables of hourly mean
116 values of the H component from Huancayo or their microfilmed copies obtained from
117 the World Data Center for Solar-Terrestrial Physics, Boulder, and scanned as digital
118 images. To this end, about 19 years of HUA data have been digitised recently by us by
119 typing from the digital images, corresponding to more than 150,000 hourly mean values
120 for the H component with 1 nT resolution. However, for 1992 to 1997 no such
121 handwritten data exists and this gap could not be filled in.

122 During some periods, mainly 1964 to 1967 and some shorter intervals in the end of the
123 1960ies, there is now both newly digitised data as well as already existing values from
124 the World Data Centre (WDC) for Geomagnetism, Kyoto, available. The data from these
125 two sources are not always identical, and, except for the period August 1966 to
126 December 1966 (here, the data from WDC showed unexpectedly large amplitudes in the
127 daily variation when normalised to the solar flux), we used the data from the WDC for
128 the analysis here (Matzka et al., 2017).

129

130 Daily total sunspot numbers R were taken from WDC-SILSO, Royal Observatory of
131 Belgium, Brussels (http://www.sidc.be/silso/DATA/SN_d_tot_V2.0.txt), dataset after
132 revision from July 1st, 2015 (SISLO, 2017). The Kp index and the International Quiet
133 Days were taken from GFZ German Research Centre for Geosciences, Potsdam
134 (<ftp://ftp.gfz-potsdam.de/pub/home/obs/kp-ap/>). The definitive Dcx index (Mursula
135 and Karinen, 2005; Mursula et al, 2008) was taken from University Oulu

136 (<http://dcx.oulu.fi>). The Dcx index is an extended (back to 1932) and seasonally
137 corrected version of the Dst index. Solar radio flux values F10.7 are provided from
138 Natural Resources Canada (<http://www.spaceweather.ca/solarflux/sx-en.php>), we have
139 used daily observed F10.7 values.

140

141 **Calculation**

142 We performed two independent analyses to calculate the annual mean of the daily
143 variation amplitude and then subtracted the solar cycle variation from it. This is done
144 for the years 1935 to 1985, when inclination at Huancayo was rather constant (Fig. 1a),
145 but magnetic field strength was decreasing (Fig. 1b).

146

147 In the first approach, labelled A_1 , the Dcx index was subtracted from the H component to
148 remove the effect of the magnetospheric ring current from the data. To characterise the
149 amplitude ΔH of the daily variation, for every day a quiet night time value was
150 subtracted from the mean of H for the time from 11 to 14 LT. The quiet night time values
151 were determined for each month by taking the mean of the night time values (from 23 to
152 03 LT) for the 5 International Quiet Days published by GFZ. Thus the geomagnetic main
153 field was removed from the data and ΔH represents the amplitude of both the Sq and the
154 EEJ signal. Only days with $\sum Kp \leq 18$ were selected to calculate the annual mean of ΔH .

155

156 In the next step of approach A_1 , the linear regression between annual means of ΔH and
157 the annual means of daily total sunspot number R was determined and subtracted from
158 the annual means of ΔH . This yields annual means of the residual $\Delta H_r = \Delta H - \Delta H_p$ (ΔH_p
159 are predicted from R by the obtained linear fit) independent from solar cycle variations.

160

161 In the second approach, denoted here A_2 , first the Dcx index was subtracted from the H
162 component and hourly mean values were kept only for periods with $Kp < 3$. Then, quiet
163 night time levels were determined by calculating the median value of H from 23 LT to
164 04LT (the same approach as used by Yamazaki (2010)) for each night and linearly
165 interpolated between the nights to have continuous time series of quiet night time
166 values. The quiet night time levels were subtracted from the H component, removing the
167 main field and yielding an hourly mean value time series representative of the EEJ and
168 Sq signal and being close to zero at night time. For each day, the daily maximum was
169 reconstructed from these hourly mean values by fitting a cubic spline to the 7 values

170 around noon (09:30 LT to 15:30 LT). The maximum of the spline fit then represents ΔH .
171 Annual mean values of ΔH were then calculated.

172

173 In the second step of approach A_2 , the linear regression between annual means of ΔH
174 and the annual means of square root of a reconstruction of solar flux F10.7 was
175 determined and used to predict ΔH_p , which was subtracted from the annual means of ΔH
176 to yield annual means of the residual of ΔH . Since F10.7 values only go back to 1947, and
177 the relationship between F10.7 and sunspot number in Siddiqui et al. (2015) is only
178 valid for the superseded (pre 2015) sunspot time series, we have updated the
179 relationship for reconstructing daily observed F10.7 from the revised daily total sunspot
180 number:

181

$$182 \quad (1) \quad F10.7 = 0.59 * R + 66.65$$

183

184 and use this to calculate annual means of F10.7 from 1935 to 1946.

185

186 **Results**

187 The annual means of ΔH for 1935 to 1985 calculated by approach A_1 and A_2 are shown
188 in Fig. 1c and Fig. 1d, respectively. Both show clearly the signatures of 5 solar maxima
189 (solar cycles 17 to 21). Approach A_1 yields lower ΔH values than approach A_2 . The same
190 can be seen in Fig. 2. Approach A_1 yields ΔH values that are one-third (for lowest solar
191 activity) to one-fourth (for highest solar activity) lower than those by approach A_2 (Fig.
192 2). There exists a well-defined linear relationship between the results of the two
193 approaches

$$194 \quad (2) \quad \Delta H(A_1) = 0.84 * \Delta H(A_2) - 14.0 \text{ nT}$$

195 with a linear correlation coefficient $r = 0.99$.

196

197 Both approaches show a linear relationship that predicts annual mean ΔH_p , i.e. the solar
198 cycle dependency of ΔH , from sunspot numbers R for approach A_1 and from $\sqrt{F10.7}$ for
199 approach A_2 :

$$200 \quad (3) \quad \Delta H_p \text{ (nT)} = 0.358 * R + 58$$

$$201 \quad (4) \quad \Delta H_p \text{ (nT)} = 15.22 * \sqrt{F10.7} - 39$$

202

203 Hence, ΔH_p subtracted from the corresponding ΔH (shown in Fig 1c and Fig 1d,
 204 respectively), results in the residual ΔH_r plotted in Fig 3, which show a tendency to
 205 increase with time. Plotting the same annual means of ΔH_r versus the corresponding
 206 geomagnetic main field strength shows a tendency of decreasing ΔH_r with increasing
 207 magnetic main field strength (Fig. 4).

208

209 The red lines in Figs. 3 and 4 are linear least square fits to the residuals, parameters of
 210 these fits are given in Table 1. A t-test was performed with the null-hypothesis that the
 211 slopes and intercepts are zero. In each case, the resulting p-value is smaller than $\alpha = 0.05$
 212 which leads to rejection of the null-hypothesis. Thus, we find the trends in ΔH_r to be
 213 statistically significant.

214

215 **Table 1**

216 Linear least square fit and statistical analysis.

217 -----

218	Method	slope+- std. error	95 % confidence interval	p-value
219	A_1 vs. year	0.082+-0.036 nT/yr	0.010 to 0.155 nT/yr	0.0260
220	A_2 vs. year	0.133+-0.038 nT/yr	0.056 to 0.210 nT/yr	0.0010
221	A_1 vs. field	-0.0014+-0.0006 nT/nT	-0.0027 to -0.0020 nT/nT	0.0226
222	A_2 vs. field	-0.0022+-0.0007 nT/nT	-0.0035 to -0.0008 nT/nT	0.0017

223

224 **Discussion**

225 The daily variation ΔH and the solar cycle signal dependent prediction ΔH_p are very
 226 similar in size and the residual $\Delta H_r = \Delta H - \Delta H_p$ is very small and would likely be affected
 227 by artefacts in the computation of ΔH or ΔH_p . Therefore, two independent codes using
 228 different methods A_1 and A_2 for calculating both ΔH and ΔH_p are used.

229

230 We regard approach A_1 as rather crude, but robust, as it just takes a simple mean value
 231 over three hourly mean values around local noon to determine the maximum in daily
 232 variation. Thus, we expect it to significantly underestimate the amplitude of the daily
 233 variation. Approach A_2 is more sophisticated as it approximates the hourly mean values
 234 around the maximum in the daily variation by a cubic spline and the daily variation is
 235 determined from the maximum value of the spline, yielding values at least as high as the
 236 maximum hourly mean value. We note the well-defined linear relationship (equation 2)

237 with $r = 0.99$ between the two approaches and attribute the difference in ΔH to the
238 systematic underestimation of ΔH by approach A_1 .

239

240 We present an updated reconstruction of solar flux F10.7 based on sunspot number R
241 (equation 1) and we present the solar cycle dependency of the daily variation ΔH both as
242 a function of sunspot number (e.g. Elias et al., 2010) and $\sqrt{F10.7}$ (e.g. Yamazaki and
243 Kosch, 2014) in equations 3 and 4. This makes the study comparable to earlier studies,
244 but note that the sunspot numbers have been revised in 2015 by SILSO and we use the
245 revised version.

246

247 From the time series of Huancayo, only the years 1935 to 1985 were used, as here the
248 inclination at Huancayo was rather constant between 1.92° and 2.26° , indicating that the
249 magnetic equator and the latitudinal centre of the EEJ were at distance between about
250 100 to 120 km from Huancayo. Taking the EEJ current profile determined from satellite
251 data by Lühr et al. (2004) and calculating the daily variation ΔH at ground level due to
252 the EEJ alone (neglecting Sq), this distance would correspond to a 10 % drop in ΔH
253 compared to a station exactly below the EEJ. More important here, the variability in ΔH
254 due to the slight movement of the magnetic equator at Huancayo between 1935 and
255 1985 remains within 2 % (1.7 nT). A similar variability of maximum 2.3 % can be
256 derived from models based on ground measurements of ΔH integrating the effect of the
257 EEJ and Sq (see Figure 6 in Stening (1985)). There is no resemblance between the trends
258 in the inclination I from 1935 to 1985 (Fig. 1 a) to the variations of ΔH_r versus time in
259 Fig 3. This is evidence that our results are only little, if at all affected by movements of
260 the magnetic equator.

261

262 The geomagnetic field strength decreased by 2681 nT or 9.05 % from the year 1935 ($F =$
263 29628 nT; $H = 29606$ nT) to the year 1985 ($F = 26947$ nT; $H = 26931$ nT) due to secular
264 variation of the Earth's core field (main field). Following the scaling law derived by the
265 CMIT model (Cnossen et al., 2012; Cnossen, 2016), the daily magnetic variation
266 (corresponding to ΔH) should vary with $M^{-0.7}$, with M being the Earth's magnetic field's
267 dipole moment. By running the CMIT with a dipole geomagnetic field of varying
268 strength, the effect of field strength on external current systems can be investigated
269 without any effects from changes in field geometry. In reality, the Earth's magnetic field
270 is more complex, and Huancayo is located in a large-scale main field anomaly, the South

271 Atlantic Anomaly, that controls its magnetic field strength and geometry. Since the Sq
272 and EEJ current systems are controlled by large-scale processes in the ionosphere, we
273 assume here that the magnetic field strength F in the (large-scale) region around
274 Huancayo affects our ΔH with the same scaling law, i.e. ΔH proportional $F^{-0.7}$. For
275 simplicity, we assume the magnetic field change in the source region (the ionospheric
276 current system) to be the same as measured on ground at Huancayo (F decreases by
277 9.049 %). Indeed, a large-scale area around Huancayo is affected by the South Atlantic
278 Anomaly and shows a rather homogeneous decreasing magnetic field strength for the
279 investigated time period (Figure 1 in Cnossen and Richmond, 2013). At Huancayo, the
280 magnetic equator somewhat changes its orientation with time (Figure 2 in Cnossen and
281 Richmond, 2013), but for the reasons given above we assume no influence on the
282 amplitude of the daily variation. Thus, the change in ΔH predicted by the CTIM model, i.e.
283 using a scaling law of $F^{-0.7}$ and F changing from 29628 nT to 26947 nT} amounts to an
284 increase by 6.9 %. in the time span investigated.

285

286 The observed change in daily variation ΔH is obtained by multiplying the slope from
287 Table 1 with the main field change of 2681 nT, yielding 3.9 nT for A_1 and 5.9 nT for A_2 .
288 For comparison with the model predicted change in ΔH , we translate the observed
289 trends into percentage values by dividing the magnitude of variation with the mean
290 value of the observed ΔH (97 nT and 133 nT, respectively), and obtain 4.0 % for A_1 and
291 4.4 % for A_2 .

292

293 Thus, two independent analyses, A_1 and A_2 , were performed with two independent
294 codes and successfully validated against each other. The good agreement between A_1
295 and A_2 lends confidence to the employed methods for calculating ΔH and ΔH_p . Our
296 method to calculate the percentage changes in ΔH for a given period is similar in
297 principle to the method used by Elias et al. (2010): calculation of residuals, linear fit of
298 residuals including t-test of significance, and normalisation on the mean value of ΔH .

299

300 Our results for the change in ΔH (4.0 and 4.4 % decrease, respectively) have the same
301 sign and are in the same order as the scaling law model prediction, but somewhat
302 smaller. Adding one standard error to the result of A_2 yields 5.8 %, which is close the 6.9
303 % predicted from the scaling law. However, the observed trends could also be affected
304 by variations in tidal forcing as well as in neutral temperature, density, and composition,

305 which have not been accounted for in the physics-based modelling efforts. Possible
306 effects of the different processes have been reviewed, e.g. in Cnossen (2012).

307

308 When comparing our results to previous studies on Huancayo data, there are several
309 limitations. Sellek (1980) didn't find long-term trends in solar daily variation at
310 Huancayo, but he used only a relatively short dataset of 14 years (1948 to 1961).

311 Shinbori et al. (2014) investigated Huancayo data from the World Data Centres for 1947
312 to 2009 (with data gaps as shown in Fig 1. d), but did not specify a trend because of the
313 data gaps (pers. comm. A. Shinbori, 2017). In contrast, in the analysis of the full dataset
314 including the newly digitised observations presented here, a significant negative trend
315 of the signal with increasing geomagnetic field strengths could be identified.

316

317 **Conclusion**

318 We have analysed Huancayo geomagnetic observatory data hourly mean values from
319 1935 to 1985 to determine the annual means of the amplitude ΔH of the quiet daily
320 variation of the H component, which is proportional to the east-west oriented equatorial
321 ionospheric current system. These currents consist of the solar quiet current system and
322 the equatorial electrojet. To this end, we digitised some 19 years of hourly mean values
323 previously not available for this key equatorial station. This data is available as a data
324 publication (Matzka et al., 2017), and will be submitted to the World Data Centres.

325

326 For this analysis, we took advantage of the strong decrease in main field strength at
327 Huancayo (due to the South Atlantic Anomaly) and of the unique, long time series of
328 Huancayo geomagnetic observatory. We selected a time interval, 1935 to 1985, in which
329 changes of the magnetic equator relative to the observatory were negligible for our
330 study. The analysis is valid under the assumption, that the slight change in the
331 orientation of the magnetic equator did not affect the amplitude ΔH of the quiet daily
332 variation.

333

334 The sensitivity of ΔH to solar cycle variations (in terms of sunspot numbers and solar
335 flux F10.7) and to changes of the geomagnetic main field strength (due to secular
336 variation) was determined. The sensitivity to changes in main field strength determined
337 from Huancayo data are similar, but somewhat (one-third) lower than the changes
338 predicted from the physics based CMIT model (Cnossen, 2016). We note that possible

339 effects from variations in tidal forcing and in neutral temperature, density, and
340 composition have not been accounted in the physics-based modelling and could be
341 responsible for differences in model and observation.

342

343

344 **Acknowledgements**

345 We acknowledge the geomagnetic observatory Huancayo, Instituto Geofísico del Perú,
346 and WDC for Geomagnetism, Kyoto, for hourly mean values. Sunspot data are from
347 WDC-SILSO, Royal Observatory of Belgium, Brussels. Kp-index and International Quiet
348 Days are from GFZ German Research Centre for Geosciences, Potsdam. The results
349 presented in this paper use Dcx indices provided by the Dcx server of the University of
350 Oulu, Finland, at <http://dcx.oulu.fi>. F10.7 was taken from Natural Resources Canada
351 (<http://www.spaceweather.ca/solarflux/sx-en.php>).

352

353 **Contributions**

354 JM designed the study, wrote the manuscript, and contributed to digitizing and analysing
355 HUA data. TAS performed the analysis (A_1) and made the graphs. HL digitized HUA data
356 and performed the analysis (A_2). CS contributed to designing the study. OV contributed
357 to designing the study and provided HUA data.

358

359

360 **Funding Sources**

361 This work was supported by Deutsche Forschungsgemeinschaft (grant number MA-
362 2578-4-1).

363

364 **References**

365

366 Chapman, S., 1951. The equatorial electrojet as detected from the abnormal electric
367 current distribution above Huancayo, Peru, and elsewhere, Arch. Met. Geoph. Biokl. A,
368 Band IV, pp. 368-390

369

370 Choque, E., Ishitsuka, J., Yumoto, K., Veliz, O., Rosales, D., 2014. MAGDAS I and II
371 magnetometers in Peru. Sun and Geosphere, 9 (1), pp. 27-30.

372

373 Chulliat, A., Matzka, J., Masson, A., Milan, S. E., 2016. Key Ground-Based and Space-Based
374 Assets to Disentangle Magnetic Field Sources in the Earth's Environment. - Space Science
375 Reviews, doi:10.1007/s11214-016-0291-y (online)
376

377 Cnossen, I., 2012. Climate change in the upper atmosphere. In: Liu, G. (ed.), Greenhouse
378 gases: Emission, Measurement, and Management. InTech, pp. 315-336, ISBN 978-953-
379 51-0323-3
380

381 Cnossen, I., Richmond, A.D., Wiltberger, M., 2012. The dependence of the coupled
382 magnetosphere-ionospherethermosphere system on the Earth's magnetic dipole
383 moment. J. Geophys. Res. 117, A05302, doi:10.1029/2012JA017555
384

385 Cnossen, I., Richmond, A.D., 2013. Changes in the Earth's magnetic field over the past
386 century: Effects on the ionosphere-thermosphere system and solar quiet (Sq) magnetic
387 variation. J. Geophys. Res., Space Physics, 118, pp. 849–858, doi:10.1029/2012JA018447
388

389 Cnossen, I., 2016. The Impact of Century-Scale Changes in the Core Magnetic Field on
390 External Magnetic Field Contributions. Space Sci. Rev. DOI 10.1007/s11214-016-0276-x
391

392 Cnossen, I., Matzka, J., 2016. Changes in solar quiet magnetic variations since the
393 Maunder Minimum: A comparison of historical observations and model simulations. J.
394 Geophys. Res., 121, 10, pp. 10,520-10,535.
395

396 de Haro Barbas, B.F., Elias, A.G., Cnossen, I, Zossi de Artigas, M., 2013. Long-term changes
397 in solar quiet (Sq) geomagnetic variations related to Earth's magnetic field secular
398 variation. J. Geophys. Res. Space Physics, 118, pp. 3712–3718, doi:10.1002/jgra.50352
399

400 Elias, A.G., Zossi de Artigas, M., de Haro Barbas, B.F., 2010. Trends in the solar quiet
401 geomagnetic field variation linked to the Earth's magnetic field secular variation and
402 increasing concentrations of greenhouse gases. J. Geophys. Res., 115, A08316.
403

404 Glassmeier, K.H., Vogt, J., Stadelmann, A., Buchert, S., 2004. Concerning long-term
405 geomagnetic variations and space climatology. Ann. Geophys. 22(10), pp. 3669–3677
406

407 Lühr, H., Maus, S., Rother, M., 2004. Noon-time equatorial electrojet: Its spatial features
408 as determined by the CHAMP satellite. *J. Geophys. Res.*, 109, A01306,
409 doi:10.1029/2002JA009656
410

411 Macmillan, S., Droujinina, A. 2007. Long-term trends in geomagnetic daily variation.
412 *Earth Planets Space*, 59, pp. 391–395
413

414 Marriott, R.T., Richmond, A.D., Venkateswaran, S.V., 1979. The quiet-time equatorial
415 electrojet and counter-electrojet. *J. Geomag. Geoelectr.*, 31, pp. 311-340, 1979
416

417 Matzka, J., Chulliat, A., Manda, M., Finlay, C.C., Qamili, E., 2010. Geomagnetic
418 observations for main field studies: From ground to space. *Space Sci. Rev.*, 155, pp. 29-
419 64, doi:10.1007/s11214-010-9693-4
420

421 Matzka, J., Lilienkamp, H., Siddiqui, T.A., Veliz, O., 2017. Hourly Mean Values
422 Geomagnetic Observatory Huancayo (HUA), 1935 to 1985. V. 1. GFZ Data Services.
423 <http://dx.doi.org/10.5880/GFZ.2.3.2017.001>.
424

425 Mursula, K., Holappa, L., Karinen, A., 2008. Correct normalization of the Dst index.
426 *Astrophys. Space Sci. Trans.* 4, pp. 41–45.
427

428 Mursula, K., Karinen, A., 2005. Explaining and correcting the excessive semiannual
429 variation in the Dst index. *Geophys. Res. Lett.* 32, pp. 14107–14111.
430

431 Schlapp, D.M., Sellek, R., Butcher, E.C., 1990. Studies of worldwide secular trends in the
432 solar daily geomagnetic variation. *Geophys. J. Int.* 100, 469–475.
433

434 Sellek, R., 1980. Secular trends in daily geomagnetic variations. *J. Atm. Terr. Phys.*, 42,
435 pp. 689-695.
436

437 SILSO, 2017. SISLO, World Data Center - Sunspot Number and Long-term Solar
438 Observations, Royal Observatory of Belgium, on-line Sunspot Number catalogue:
439 <http://www.sidc.be/SILSO/>, 1935-1985
440

441 Shinbori, A., Koyama, Y., Nose, M., Hori, T., Otsuka, Y., Yatagi, A., 2014. Long-term
442 variation in the upper atmosphere as seen in the geomagnetic solar quiet daily variation.
443 Earth Planets Space, 66, 155.
444

445 Siddiqui, T., Lühr, H., Stolle, C., Park, J., 2015. Relation between stratospheric sudden
446 warming and the lunar effect on the equatorial electrojet based on Huancayo
447 recordings". Ann. Geophys., 33, pp. 235–243.
448

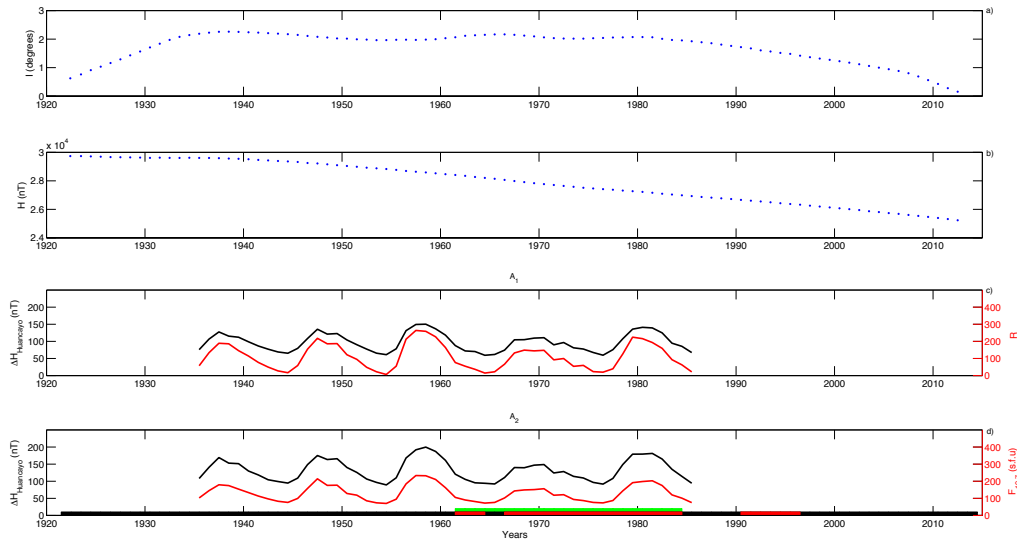
449 Stening, J.R., 1985. Modeling the equatorial electrojet. J. Geophys. Res., 90, A2, p. 1705-
450 1719.
451

452 Yamazaki, Y., Yumoto, K., Uozumi, T., Abe, S., Cardinal, M.G., McNamara, D., Marshall, R.,
453 Shevtsov, B.M., Solovyev, S.I., 2010. Reexamination of the Sq-EEJ relationship based on
454 extended magnetometer networks in the east Asian region. J. Geophys. Res., 115,
455 A09319.
456

457 Yamazaki, Y., Kosch, M.J., 2014. Geomagnetic lunar and solar daily variations during the
458 last 100 years. J. Geophys. Res., 119, 8, p. 6732-6744.
459
460
461

462 **Figure captions**

463



464

465 **Fig 1.** Annual means of geomagnetic inclination I (panel a) and horizontal component H

466 (panel b) measured at Huancayo, Peru. Annual means of the amplitude ΔH of the daily

467 magnetic variation in the H component from 1935 to 1985 calculated with our approach

468 A_1 (together with annual means of sunspot number R , panel c) and our approach A_2

469 (panel d, together with annual means of solar flux $F_{10.7}$ in $\text{s.f.u} = 10^{-22} \text{ Wm}^{-2}\text{Hz}^{-1}$).

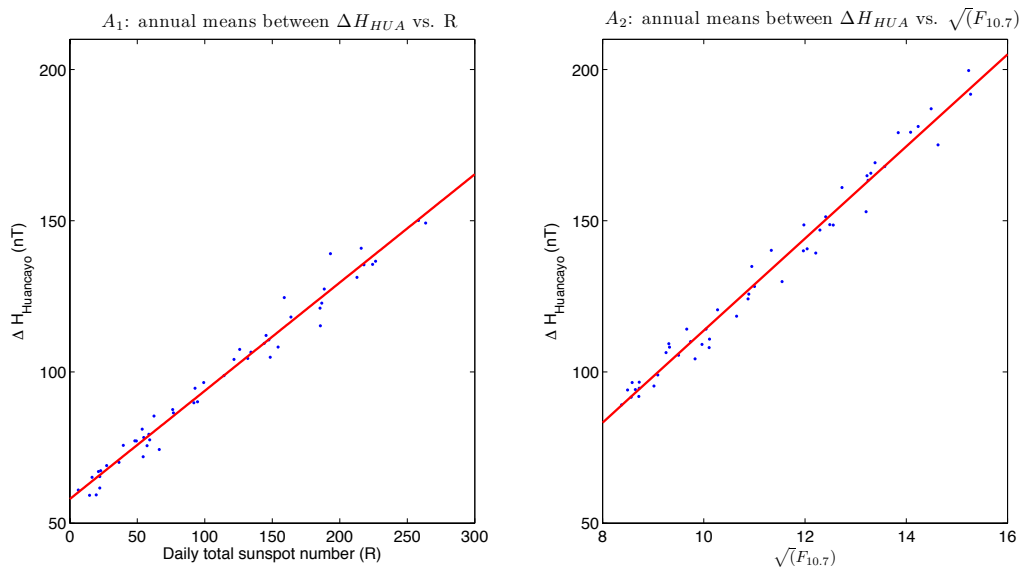
470 Periods with hourly mean values of Huancayo magnetic recordings available at the

471 World Data Centres are marked by black horizontal bars at the bottom of panel d, data

472 gaps indicated by red. The green horizontal bar indicates the newly digitised hourly

473 mean values presented in this study.

474



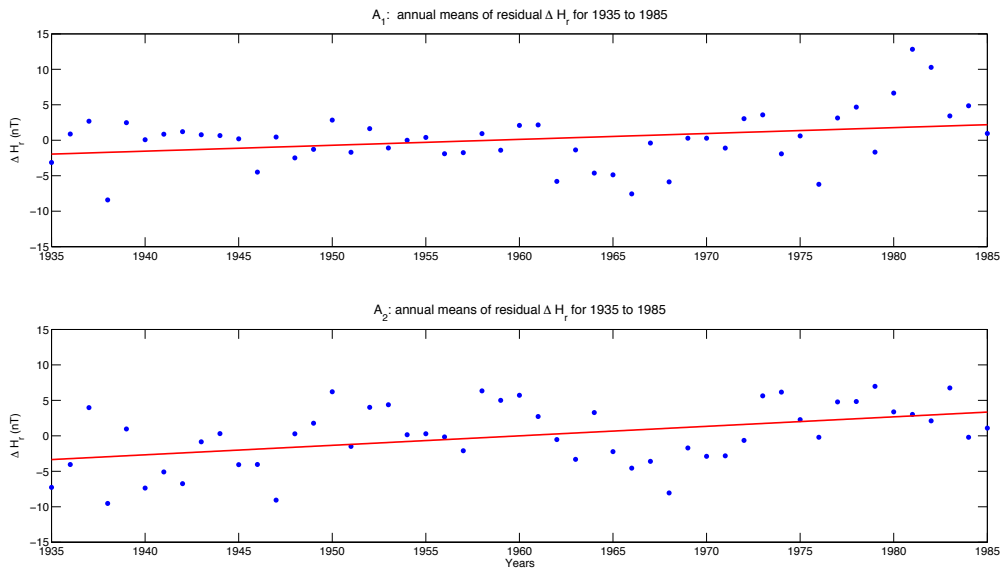
475

476 **Fig. 2.** Annual means of daily variation ΔH from approach A_1 versus annual mean of

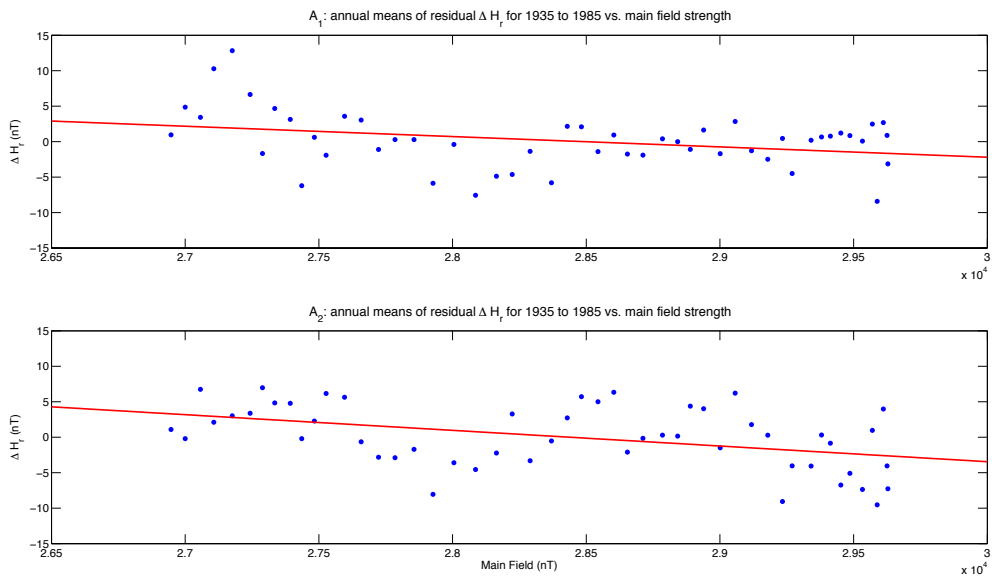
477 daily total sunspot number R (left panel) and from approach A_2 versus annual mean of

478 $\sqrt{F_{10.7}}$ (right panel). The red lines are linear least square fits (see equations 3 and 4,

479 respectively).



481
 482 **Fig 3.** Annual means $\Delta H_r = \Delta H - \Delta H_p$ residual for Huancayo 1935 to 1985 for approach A_1
 483 (upper panel) and approach A_2 (lower panel). The red lines are least square fits (see
 484 Table 1).
 485



486
 487 **Fig 4.** Annual means $\Delta H_r = \Delta H - \Delta H_p$ residual for Huancayo 1935 to 1985 versus main
 488 field strength for approach A_1 (upper panel) and approach A_2 (lower panel). The red
 489 lines are least square fits (see Table 1).